Measuring significant inhomogeneity and anisotropy in indoor convective air turbulence in the presence of 2D temperature gradient

E Mohammady Razi[1] and Saifollah Rasouli[1,2]

[1] Department of Physics, Institute for Advanced Studies in Basic Sciences (IASBS), Zanjan 45137-66731, Iran
[2] Optics Research Center, Institute for Advanced Studies in Basic Sciences (IASBS), Zanjan 45137-66731, Iran

E-mail: rasouli@iasbs.ac.ir

Abstract

Using a novel set up, experimental study of the statistical properties of a light beam propagating horizontally through indoor convective air turbulence in the presence of a 2D temperature gradient (TG) is presented. A laser beam enters a telescope from its back focal point by virtue of an optical fiber and is expanded and recollimated by it and then passes through the turbulent area. Then the beam enters another telescope's aperture. A mask consisting of four similar widely separated small subapertures was installed in front of the second telescope's aperture. The subapertures were equidistant from the optical axis of the telescope and located at the corners of a square. A flat plane heater is used to produce a vertical TG in the medium. Due to the limited width of the heater, a horizontal component for the TG appeared. Near the focal plane of the second telescope, four distinct images of the source are formed and recorded by a CCD camera. Due to the turbulence all the images (spots) in the successive frames fluctuate. Using the four spot displacements we have calculated the fluctuations of the angle of arrival (AA) over the subapertures. The statistical properties of the optical turbulence are investigated using variance analysis of the AA component fluctuations at horizontal and vertical directions over the subapertures for different temperatures of the heater at different heights of the beam path from the heater. Experimental results show that when the heater is turned off, the variances of horizontal and vertical components of the AA fluctuations are approximately equal to zero over all the subapertures. When it is turned on, the variance of the horizontal component of the AA fluctuations over all of the subapertures are larger than those from the vertical one. In addition, in this case, we find a significant dependence of the variance of the AA components on the height from the heater.

S Online supplementary data available from stacks.iop.org/JOpt/16/045705/mmedia

(Some figures may appear in colour only in the online journal)

1. Introduction

Various models have been proposed to study of the turbulence: from the Kolmogorov model without providing an analytical expression of typical scale parameters, to the Tatarskii and the von Karman models with finite inner and outer scales (the smallest and largest scales of the turbulence, respectively) [1]. These two latter models were combined in the von Karman–Tatarskii model, sometimes called the modified von Karman model. In all these models it is proposed that the turbulence is isotropic and homogeneous. Atmospheric turbulence and controlled indoor air turbulence are among the important topics in the study of turbulence. Experimental studies show that the statistics of wavefront phase propagation through the atmosphere do not always guarantee homogeneity and isotropy of the atmospheric turbulence and do not always obey the power laws associated with the Kolmogorov model of atmospheric turbulence [2–8]. As the Earth's surface is the atmosphere's primary heat source, and as the different parts of the Earth's surface can absorb different values of the solar energy, it is reasonable to have changes in the temperature with distance in vertical and horizontal directions near the Earth's surface. Due to the Earth's surface profile and the existence of non-constant and non-equal temperature gradients in the vertical and horizontal directions at various altitudes and locations, it is reasonable to expect that for a light beam propagating through atmospheric turbulence especially near to the Earth's surface on a horizontal path, the homogeneity and isotropy of the atmospheric turbulence may be violated. To the best of our knowledge, until now there have been no comprehensive studies on the effect of a 2D temperature gradient (TG) on the statistical properties of a light beam propagating through atmospheric turbulence or through indoor convective air turbulence. However, it is worth mentioning that in different experimental works, some aspects of homogeneity and/or isotropy of the atmospheric turbulence and indoor convective turbulence have been studied with different methods, such as radar scatter from the atmosphere [9], angle of arrival variances dependence on the aperture size for indoor convective turbulence [10], investigation of the atmospheric turbulence spatial structure [11], measuring the relative dancing of two parallel beams propagating through the atmosphere [12, 13], measuring the laser beam wandering variance with the turbulent path length [14], and studying the velocity structure function at the atmospheric turbulence using time series from a single hot wire pair [15]. It is clear that the first step can be a case study to answer the following question, 'Can and how does a 2D TG play a role in the inhomogeneity and anisotropy of the air turbulence in a controlled, laboratory experiment?' The next step may be the study of the atmospheric turbulence. This study is the subject of future research at IASBS especially using the moiré based methods [16–20].

In this work we report the measurement of significant inhomogeneity and anisotropy in the statistical properties of indoor convective air turbulence in the presence of a 2D TG using a new set up. The experimental set up consists of a laser, an optical fiber with suitable connectors, a pair of telescopes,
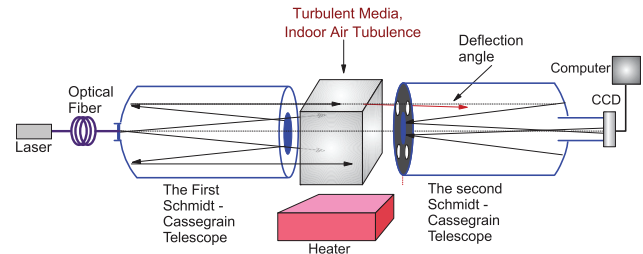

Figure 1. Schematic diagram of the experimental setup.

a heater with controlled temperature, a CCD camera, and a computer, as shown in figure 1. The laser beam enters the first telescope by virtue of the optical fiber and suitable connectors and is expanded and recollimated by it and passes through the turbulent area. Then the beam enters the second telescope's aperture. The use of two telescopes creates a large collimated beam and it can be used for studying the spatial and temporal properties of wavefronts. A mask consisting of four small similar circular subapertures all located on the corners of a square, is installed at the entrance pupil of the second telescope and its center lies on the optical axis of the telescope. The CCD camera is located slightly outside the focal plane of the second telescope so that each subaperture produces an image well separated from all of the other images produced by the mask. Due to the turbulence, successive images fluctuate. Using the image fluctuations, we have calculated the fluctuations of the angle of arrival (AA). A flat plane heater with controlled temperature is used to produce a vertical TG in the medium (see figure 1). Due to the limited width of the heater's surface, a horizontal component for the TG appeared. It is worth mentioning that, in this experiment, the value of horizontal component of the TG is directly affected from the value of the vertical component of the TG and both of them are affected from the heater's temperature. In addition it is reasonable that, these two components of the TG to be not equal. Using a set of temperature sensors, we detected such 2D temperature distribution above the heater when it is turned on. The heater's temperature can be changed from the room temperature to 150 °C with a fluctuation less than 1 °C.

In this study convective air turbulence is the subject of the work and kinematic turbulence motion of the air particles is guaranteed by the convection. In comparing with a similar indoor experiment proposed by Masciadri and Vernin [21] in which the kinematic motion is produced by the air flow, here the kinematic factor is produced simply by the background conditions of the indoor air particles. In our set up, the convective air flow initially can originate from the replacement of the cold air coming from all sides of the heater to the hot area over the heater.

The statistical properties of the optical turbulence are investigated using variance analysis of the AA component fluctuations at horizontal and vertical directions over the subapertures on the entrance pupil of the second telescope. Experimental results show that, when the heater is turned off, the variance of the vertical and horizontal components of the AA fluctuations are equal and turbulence may be considered isotropic, but When it is turned on, the variance

of the horizontal component of the AA fluctuations over all of the subapertures are larger than those from the vertical one. In addition, when the heater is turned on, we find significant dependence of the variance of the AA components on the height of the beam path from the heater. A similar anisotropy was also observed for the laser beam wandering variance at the indoor convective turbulence by Funes *et al* [14].

2. Method of data analysis

We assume that a plane wave emerges from the first telescope and passes through the turbulent area, then the deformed wavefront enters to the second telescope's aperture. The CCD camera is located slightly outside the focal plane of the second telescope so that each subaperture produces an image well separated from all of the other images produced by the mask. In the experiment, focal length of the second telescope is 2 m and the CCD camera is located 1 cm outside from the focal plane of the second telescope. In the formulation of the AA calculations from the image displacements, for simplicity we consider image displacements in the focal plane instead of in the real image plane. In this regard, to compensate the out-of-focus effect on the AA calculations, value of 2.01 m for the focal length of the second telescope is used. Now, over each subaperture the deformed wavefront has a local AA component, for example, in the x-direction as

$$\alpha_{i_x} = \frac{l_x(x_{g_i} - \overline{x}_{g_i})}{f_2}, \qquad i = 1, 2, 3, 4, \tag{1}$$

where, l_x, x_{g_i}, $\overline{x}_{g_i}$, and f_2 are the pixel size in the x-direction on the image plane, x component of the center of image of the ith subaperture, the mean position of the center of the image in the x-direction, and the second telescope's focal length, respectively. The center of the image formed by each subaperture is defined as the center of gravity also called the centroid. Each centroid is related to the wavefront gradients averaged over the corresponding subaperture. If $I(x, y)$ is the light intensity distribution on a spot image at a plane close to the telescope's focal plane (with background subtracted), its centroid in the x-direction is defined by

$$x_g = \frac{1}{I_{\text{tot}}} \int x I(x, y) \, \mathrm{d}x \, \mathrm{d}y, \tag{2}$$

where I_{tot} is the total flux (the integral of image intensity). In practice, for the discrete (pixelized) CCD image, the integral may be replaced by the sum over all pixels.

Two centroiding methods, thresholding and windowing, are commonly used in practice. In this work we have used the windowing method. In the windowing method, only the pixels within some radius from the image center are taken into account. In this work, we used a circular window with a radius equal to the radius of the first dark ring in Airy image for all of the images of the subapertures. We take the coordinates of the brightest pixel as the window's center.

As it was mentioned above, image separation is achieved by locating the detector slightly out-of-focus with respect to the full-aperture optical system (the second telescope). As we have

recorded out-of-focus images, the centroid measurements are biased by the defocus. In addition, the growing turbulence is deteriorated recorded images, which is a serious limiting issue and the centroid measurements are also biased by this effect. To remove the unwanted effects of these biases, the defocus and the growing turbulence, we have computed the Strehl ratio of all of the recorded spot images. Data with Strehl ratio below 0.55 are not used in the statistical analysis. In practice, for a heater's temperature below 100 °C there is no serious bias, but at the higher heater's temperature for example at 120 °C in a set of 5000 successive recorded images about 170 images have a Strehl ratio below 0.55 and we are not used them in the statistical analysis.

The time series of the horizontal and vertical image centroids, or AA fluctuations, for all of the subapertures are calculated. Using the time series of the image centroids, the variances of the AA component fluctuations at the horizontal and vertical directions over the subapertures are obtained. In this work, statistical error of the variance of the AA component fluctuation measurements is calculated from [22]

$$\delta\sigma_\alpha^2 = \sqrt{\frac{2}{N-1}}\sigma_\alpha^2, \tag{3}$$

where, N is the number of data and σ_α^2 is the variance of the AA component fluctuations; by considering $N = 5000$ and $\sigma_\alpha^2 \simeq 10^{-11}$ rad^2, typical statistical error of the variance of the AA component fluctuation measurement is 10^{-13} rad^2.

The uncertainty or error in the AA measurement can be found by using the rules of propagation of uncertainties. If the original uncertainties are independent and random, the uncertainties are added in quadrature [23]. Therefore, the error of the wavefront slop measurement over each of subapertures is calculated from

$$\frac{\delta\alpha_x}{\alpha_x} = \sqrt{\left(\frac{\delta l_x}{l_x}\right)^2 + \left(\frac{\delta(x_g - \overline{x}_g)}{(x_g - \overline{x}_g)}\right)^2 + \left(\frac{\delta f_2}{f_2}\right)^2}, \tag{4}$$

where δ shows the measurement error of the corresponding parameter.

As x_g and $\overline{x}_g$ are determined from the integral of image intensity and the mean position of the center of the image in successive frames, respectively, their errors are determined by $\delta x_g = \frac{\sigma_{x_g}}{\sqrt{n}}$ and $\delta\overline{x}_g = \frac{\sigma_{\overline{x}_g}}{\sqrt{N}}$. n is the number of pixels are used for determining the center of intensity gravity in each image and N is the total number of images are used for determining the mean position of the center of the image. For the reported experimental data, these errors are determined $\delta x_g = 0.21$ pixel and $\delta\overline{x}_g = 0.04$ pixel. In this work, we have used $l_x = 5.2 \times 10^{-6}$ m, $f_2 = 2.01$ m; by considering δl_x is negligible, $(x_g - \overline{x}_g) = 30$ pixel, $\delta(x_g - \overline{x}_g) = 0.2$ pixel, and $\delta f_2 = 5$ mm, from equation (3), value of $\frac{\delta\alpha_x}{\alpha_x} = 7.1 \times 10^{-3}$ is obtained. Also, by using equation (1), the minimum measurable AA fluctuations is determined to be 7.2×10^{-7} rad or 0.15 arc s. A similar relation can be used for the local AA component in the y-direction. Of course, it is worth remembering that, values of $\alpha_{x,y}$ and $\sigma_{\alpha_{x,y}}^2$ are changed as functions of the heater's temperature, respectively. In the above presented error calculations, the heater's temperature 40 °C is presumed.

3. Experimental work

Schematic diagram of the experimental setup is shown in figure 1. In the experiment, the second harmonic of a CW diode pumped Nd–YAG laser beam enters the first telescope (the 14 in Celectron Schmidt–Cassegrain telescope) by virtue of the optical fiber and is expanded and recollimated by it and passes horizontally through an indoor air turbulent area. A flat plane heater with an upper surface area of 50 cm × 100 cm is used under the light beam path to produce a vertical TG in the medium (see figure 1). The length of the heater was parallel to the path of the light beam. The heater's temperature is controlled and can be changed in a range from the room temperature 24 to 150 °C. The heater is installed on a jack and its altitude can be easily changed. In a stable condition, a horizontal component for the TG appeared due to the limited width of the heater's surface. As it was mentioned previously, the value of horizontal component of the TG is directly affected from the value of the vertical component of TG and both of them are affected from the heater's temperature. Using a set of temperature sensors, we observed that these two components of the TG are not equal. After passing through the turbulent area the beam enters the second telescope's aperture (the Meade 8 in LX200 GPS Schmidt–Cassegrain telescope). The telescopes were 150 cm apart. We used a mask consisting of four widely separated small subapertures in front of the second telescope's aperture. Adjacent subapertures were 10.16 cm apart and had a diameter of 3 cm, figure 2(a). The area between the telescopes is isolated from the other parts of the room using two plastic isolators. These plastic isolators were 100 cm apart. We used a CCD (DCC1545M—high resolution USB2.0 CMOS Camera, Monochrome) near the back focal plane of the second telescope for recording successive frames. The sampling rate was 120 frames s^{-1} and the exposure time for a frame was 1 ms. We have recorded many sets of data at different heater temperatures and at different vertical distances of the light beam path from the heater's surface. Each set of data was collected in 42 s and contained 5000 frames. To remove the unwanted effect of the telescopes' vibration modes, the telescopes were installed on suitable bases and at the data recording time, environmental vibrations were minimized. When the heater was turned off, we did not observe any difference between the statistical properties of the x and y components of the AA fluctuations. A typical recorded frame is shown in figure 2(b), where the heater's temperature and height of telescopes from the heater were 70 °C and 80 cm, respectively. The background movie of figure 2, contains 300 successive recorded frames of slightly out-of-focus image of the point source (movie 1 available at stacks.iop.org/JOpt/16/045705/mmedia). For all of the data sets, the x and y components of the AA fluctuations were calculated from the displacements of the image points. Typical time series of the x and y components of the AA fluctuations over all of the subapertures when the temperature of heater were 24 °C (the room temperature) and 70 °C are shown in figure 3. For easy comparing the AA fluctuations at two different heater's temperatures, y-axis scales are selected equal in all of the plots. For the data of figure 3, the height of telescopes from

the heater was 80 cm. It shows that, when the heater is turned on, the statistical properties of the x and y components of the AA fluctuations are different.

In figure 4 the variances of the vertical and horizontal components of the AA fluctuations over all of subapertures at the telescope's height being 80 cm from the heater at different temperatures are shown. Hereafter, $\sigma^2_{\alpha i_x}$ and $\sigma^2_{\alpha i_y}$ stand for the variances of the horizontal and vertical components of the AA fluctuations over the ith subaperture, respectively. Note that $\sigma^2_{\alpha_x}$ and $\sigma^2_{\alpha_y}$ over all of the subapertures are approximately equal at room temperature, whereas the variance of the horizontal components of AA fluctuations exceeds that for the vertical component when the heater is turned on. The plots shown in figure 4 provide direct evidence of the anisotropy of the variances of the horizontal and vertical components of the AA fluctuations induced by the value of 2D TG. Now, it is meaningful to define the anisotropy coefficient as the ratio of the variance of the horizontal to the variance of the vertical components of the AA fluctuations,

$$a_i(T) = \frac{\sigma^2_{\alpha i_x}(T)}{\sigma^2_{\alpha i_y}(T)}, \qquad i = 1, 2, 3, 4, \qquad (5)$$

where i and T indicate the subaperture number and the heater's temperature, respectively. The value of the anisotropy coefficient a is found to be larger than 1.2 for all the data of figure 4 where the heater temperature exceeds 40 °C. An error estimation is used for a_i and maximum value of $\frac{\delta(a_i)}{a_i} = 0.014$ is obtained.

To better visualize the results, all the variances of the vertical component versus the horizontal component of the AA fluctuations over all of the subapertures for the data presented in figure 4 are shown in figure 5. Here, the heater's temperature varying from the room temperature to 120 °C. A similar anisotropy was also reported for the hot-air optical turbulence generated by the forced mixing of two air flows with different temperatures by Keskin *et al* [24].

To investigate the height effect or vertical distance of the light beam path from the heat source, we have recorded several sets of data at different heights of the telescopes from the heater at a given range of heater temperature. In figure 6 the variance of the horizontal component (x component) of the AA fluctuations over all of the subapertures are shown as a function of the heater's temperature at two heights, 40 and 80 cm, of the telescopes from the heater. In addition, we observed that in a given experiment, due to the 2D TG effect the variance of similar component of the AA fluctuations over the upper subapertures is considerably smaller than its value for the lower subapertures, figure 7.

As in the case of the anisotropy coefficient, let us define an inhomogeneity coefficient as

$$\beta_j = \frac{1}{\triangle h} \frac{\sigma^2_{\alpha_j}(h + \triangle h)}{\sigma^2_{\alpha_j}(h)}, \qquad j = x, y, \qquad (6)$$

where h and $h + \triangle h$ denote the height of the beam paths from the heater. In a given experiment, one can calculate the value of β from the data of the upper and lower subapertures.
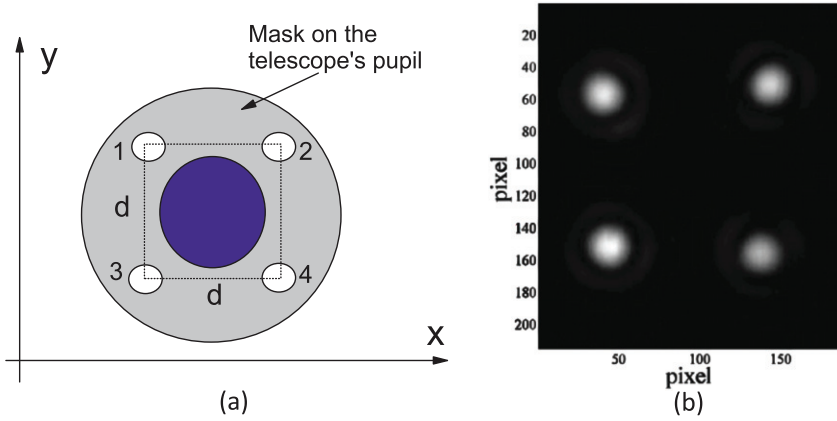
Figure 2. (a) Geometry of subapertures on the second telescope's pupil, (b) a typical recorded frame of slightly out-of-focus image of the point source. The background movie contains 300 successive recorded frames (movie 1, 1.02 MB available at stacks.iop.org/JOpt/16/04570 5/mmedia).
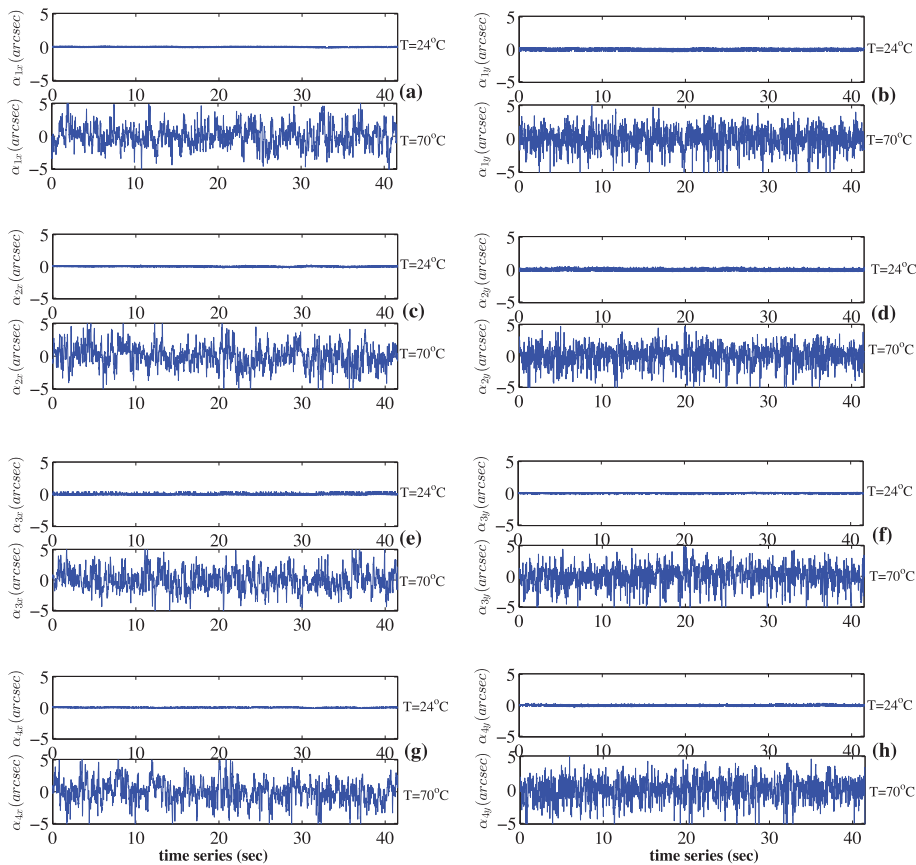

Figure 3. Vertical and horizontal components of the AA fluctuations over four subapertures on the second telescope's pupil versus the time. The height of the telescopes from the heater was 80 cm and the temperature of heater were 24 °C (the room temperature) and 70 °C.

For the data of figure 6, the values of $\beta_x = 18.5$ m^{-1} and $\beta_x = 12.2$ m^{-1} are obtained for the experiments where the height of the telescopes from the heater were 40 cm and 80 cm, respectively. An error estimation is used for β and maximum value of $\frac{\delta\beta}{\beta} = 0.017$ is obtained. Plots in figures 6 and 7 indicate that an inhomogeneity in the statistical properties of the AA fluctuations of the beam propagating perpendicular to a 2D

TG is induced by the 2D TG and its value is increased by increasing the value of the 2D TG value.

Now, a reasonable physical description for the observed anisotropy and inhomogeneity is needed. Actually, in the presented experiment, by applying a TG in the vertical direction using a heater, because of the limited dimension of the heater's surface, a new TG is also generated in the
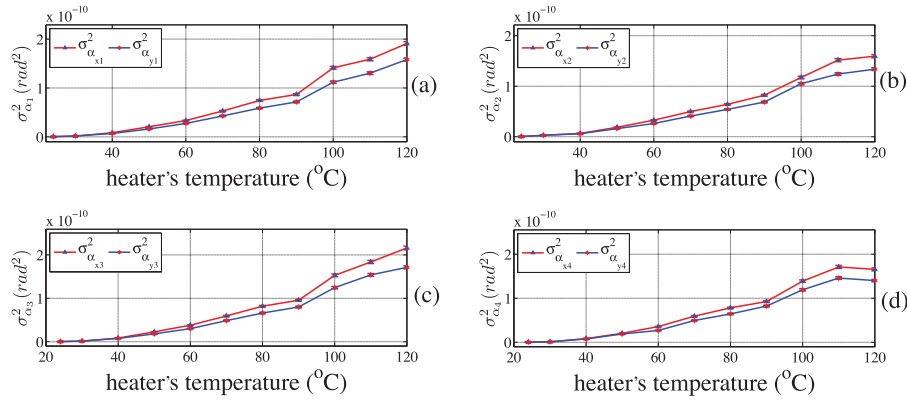
Figure 4. Variance of the vertical and horizontal components of the AA fluctuations over all of the subapertures, with the telescopes at a height of 80 cm from the heater, at different temperatures.
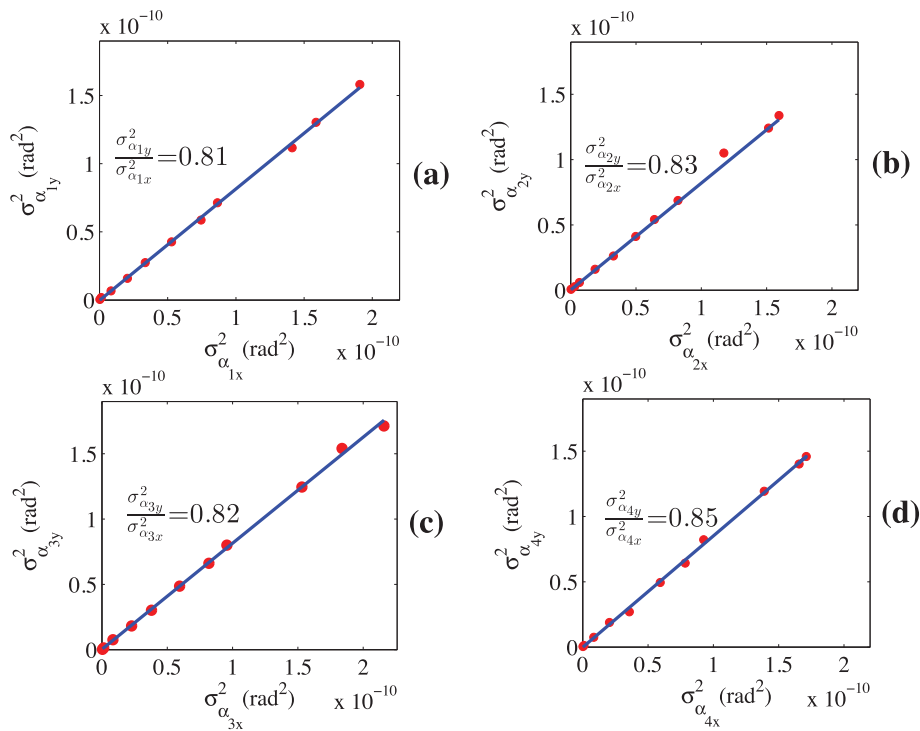

Figure 5. The variances of the vertical component versus the horizontal component of the AA fluctuations over all of the subapertures for the data presented in figure 4. The heater's temperature varying from the room temperature to 120 °C.

medium in the horizontal direction. Our measurements show that these vertical and horizontal components of the TG are not equal and it seems that the observed anisotropic turbulence can be associated to the presence of two different TGs in the vertical and horizontal directions, respectively. In addition, it is reasonable that the value of horizontal TG decreases at the higher distances from the heater. Theoretical explanation of the observed anisotropy and inhomogeneity is not the subject of this paper, but we have in mind to do so in future.

In addition, it is worth providing a connection between the indoor experiment and the case of the atmospheric turbulence. As it was mentioned, the Earth's surface is the atmosphere's primary heat source, and as the different parts of the Earth's surface can absorb different values of the solar energy, it is reasonable to have different TGs in the vertical and horizontal

direction near the Earth's surface. Other processes producing the turbulence also are same in the indoor and outdoor convective turbulences.

4. Conclusion

In this work, the effect of a 2D TG on the statistical properties of a light beam propagating horizontally through an indoor convective air turbulence is studied. For the first time, two telescopes are used face to face on both sides of a turbulent area for study of statistical properties of optical turbulence. Because of the large area of the aperture of the telescopes, this arrangement is more suitable for studying the spatial and temporal properties of wavefronts. A heater with controlled
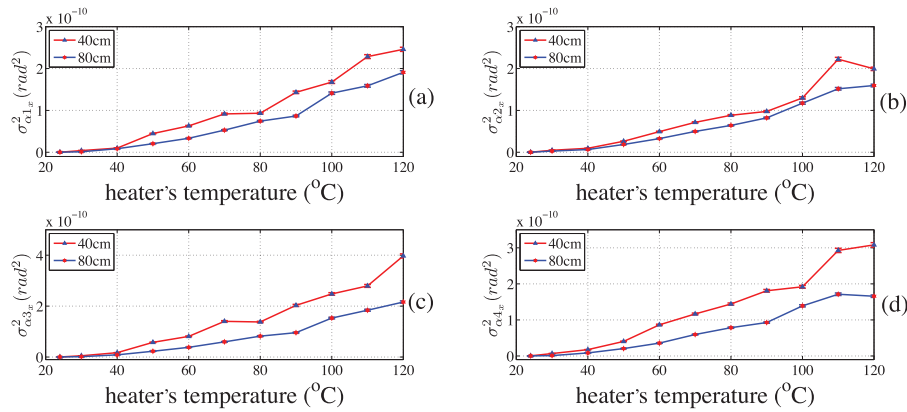
Figure 6. Variance of the horizontal component (*x* component) of the AA fluctuations over all of the subapertures as a function of the heater's temperature at two heights of the telescopes from the heater.
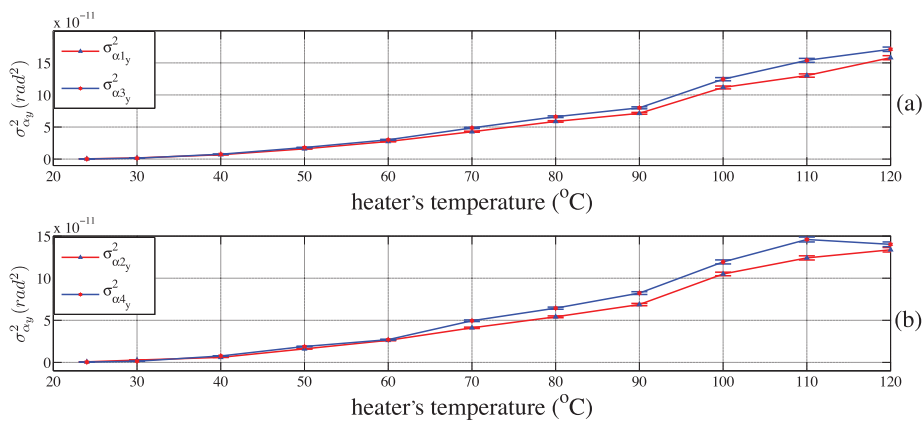

Figure 7. Variances of the vertical component of the AA fluctuations over the upper apertures and their corresponding lower subapertures.

temperature is used to produce a vertical TG in the area. Also, due to the limited width of the heater's surface, a horizontal component for the TG appeared. A mask consisting of four widely separated small apertures was installed in front of the second telescope's aperture. Using the four image spot displacements we have calculated the fluctuations of the AA components over all of the subapertures. The statistical properties of the optical turbulence are investigated using variance analysis of the AA component fluctuations at horizontal and vertical directions over the subapertures for different temperatures of the heater at different heights from the heater surface. Experimental results show that, when the heater is turned off, the variance of the vertical and horizontal components of the AA fluctuations are approximately equal to zero for all of the subapertures, but when the heater is turned on, the variance of the horizontal component of the AA fluctuations at all of the subapertures is larger than the vertical one. In addition in this case, we find a significant dependence of the variance of the AA components on the height from the heater surface. Theoretical study of the observed anisotropy and inhomogeneity can be the subject of another work, that we have in mind to do so in future at IASBS. Finally, because of the large area of the aperture of the telescopes,

the presented set up especially in conjunction with the moiré based methods [16–20] is more suitable for studying the spatial and temporal properties of wavefronts.

Acknowledgments

References

[1] Andrews L C and Phillips R L 1998 *Laser Beam Propagation though Random Media* (Bellingham, WA: SPIE Press)
[2] Dayton D, Pierson B, Spielbusch B and Gonglewski J 1992 Atmospheric structure function measurements with a Shack–Hartmann wave-front sensor *Opt. Lett.* **17** 1737–9
[3] Nicholls T W, Boreman G D and Dainty J C 1995 Use of a Shack–Hartmann wave-front sensor to measure deviations from a Kolmogorov phase spectrum *Opt. Lett.* **20** 2460–2

[4] Lukin V P 1995 Investigation of the anisotropy of the atmospheric turbulence spectrum in the low frequency range *Proc. SPIE* **2471** 347–54

[5] Gurvich A S and Belenkii M S 1995 Influence of stratospheric turbulence on infrared imaging *J. Opt. Soc. Am.* A **12** 2517–22

[6] Golbraikh E and Kopeika N S 2004 Behavior of structure function of refraction coefficients in different turbulent fields *Appl. Opt.* **43** 6151–6

[7] Rasouli S, Niry M D, Rajabi Y, Panahi A A and Niemela J J 2011 Observations of anisotropy in atmospheric turbulence by means of moiré deflectometry *The DFD11 Mtg of The American Physical Society (64th Annual Mtg Division of Fluid Dynamics) (Baltimore, MD)*

[8] Rasouli S, Niry M D, Rajabi Y, Panahi A A and Niemela J J 2014 Applications of 2-D moiré deflectometry to atmospheric turbulence *J. Appl. Fluid Mech. (JAFM)* **7** (4) (at press)

[9] Hocking W K and Hamza A M 1979 A quantitative measure of the degree of anisotropy of turbulence in terms of atmospheric parameters, with particular relevance to radar studies *J. Atmos. Sol.-Terr. Phys.* **59** 1011–20

[10] Gulich D, Funes G, Zunino L, Perez D G and Garavaglia M 2007 Angle-of-arrival variances dependence on the aperture size for indoor convective turbulence *Opt. Commun.* **277** 241–6

[11] Belenkii M S, Cuellar E, Hughes L A and Rye V A 2006 Experimental study of spatial structure of turbulence at Maui Space Surveillance Site (MSSS) *Proc. SPIE* **6304** 63040U

[12] Consortini A 1995 Sensing atmospheric turbulence by laser radiation *Opt. Rev.* **2** 308–11

[13] Consortini A, Ronchi L and Stefanutti L 2007 Investigation of atmospheric turbulence by narrow laser beams *Appl. Opt.* **9** 2543–7

[14] Funes G, Gulich D, Zunino L, Perez D J and Garavaglia M 2007 Behavior of the laser beam wandering variance with the turbulent path length *Opt. Commun.* **272** 476–9

[15] Arad I, Dhruva B, Kurien S, L'vov V S, Procaccia I and Sreenivasan K R 1998 Extraction of anisotropic contributions in turbulent flows *Phys. Rev. Lett.* **81** 5330–3

[16] Rasouli S and Tavassoly M T 2006 Application of moiré technique to the measurement of the atmospheric turbulence parameters related to the angle of arrival fluctuations *Opt. Lett.* **31** 3276–8

[17] Rasouli S and Tavassoly M T 2008 Application of the moiré deflectometry on divergent laser beam to the measurement of the angle of arrival fluctuations and the refractive index structure constant in the turbulent atmosphere *Opt. Lett.* **33** 980–2

[18] Rasouli S 2010 Use of a moiré deflectometer on a telescope for atmospheric turbulence measurements *Opt. Lett.* **35** 1470–2 and references 3–4 therein

[19] Rasouli S, Dashti M and Ramaprakash A N 2010 An adjustable, high sensitivity, wide dynamic range two channel wave-front sensor based on moiré deflectometry *Opt. Express* **18** 23906–15

[20] Dashti M and Rasouli S 2012 Measurement and statistical analysis of the wavefront distortions induced by atmospheric turbulence using two-channel moiré deflectometry *J. Opt.* **14** 095704

[21] Masciadri E and Vernin J 1997 Optical technique for inner-scale measurement: possible astronomical applications *Appl. Opt.* **36** 1320–7

[22] Frieden B R 2001 *Probability Statistical Optics and Data Testing* (Berlin: Springer)

[23] Taylor J R 1997 *An Introduction to Error Analysis the Study of Uncertainties in Physical Measurements* (Sausalito, CA: University Science Books) ISBN 0-935702-42-3 (cloth).- ISBN 0-935702-75-X (pbk.)

[24] Keskin O, Jolissaint L and Bradley C 2006 Hot-air optical turbulence generator for the testing of adaptive optics systems: principles and characterization *Appl. Opt.* **45** 4888–97